

Article

Dual-Wavelength Continuous-Wave and Passively Q-Switched Alexandrite Laser at 736.7 nm and 752.8 nm

Hongyi Lin ^{1,2,*}, Shangfeng Bao ¹, Xiao Liu ³, Shuo Song ¹, Zhiwei Wen ¹ and Dong Sun ^{1,2}

¹ School of Optoelectronic and Communication Engineering, Xiamen University of Technology, Xiamen 361024, China

² Fujian Key Laboratory of Optoelectronic Technology and Devices, Xiamen University of Technology, Xiamen 361024, China

³ School of Cultural Industries and Tourism, Xiamen University of Technology, Xiamen 361024, China

* Correspondence: 2010111010@xmut.edu.cn or linyi0714@163.com

Abstract: A dual-wavelength continuous-wave (CW) and passively Q-switched alexandrite laser based on a MoS₂ saturable absorber (SA) operating at 736.7 nm and 752.8 nm with a simple and compact 18 mm plano–plano resonator is reported. In the CW mode, the output power is 1014 mW at the linear-polarized pump power of 5.44 W, with a slope efficiency of 28.7%. In the pulsed operation, the narrowest pulse width and the maximal peak power are 154 ns and 10.6 W, respectively. This laser can be used to generate 8.71 THz-wave light based on a suitable nonlinear optical crystal.

Keywords: alexandrite laser; dual-wavelength laser; Q-switched; MoS₂

1. Introduction

The LD-pumped all-solid-state laser in the CW and/or pulsed operation has shown a variety of potential applications in the areas of holographic imaging, material processing, laser cleaning, laser display, range finding, remote sensing, photoelectric countermeasure, laser cosmetology and nonlinear frequency conversion [1,2]. The broad-spectral all-solid-state laser in the red and near-infrared band of 0.6–0.8 μm has been widely used in medical hair removal, dermatology, remote sensing lidar, microscope, photochemistry, etc. [3,4]. The alexandrite crystal is an excellent broadband tunable gain material and laser amplification medium with a long fluorescence lifetime (262 μs); high saturation energy density; wide absorption bandwidth (444, 532, 590 and 630–680 nm); small coefficient of thermal expansion ($6\text{--}7 \times 10^{-6}$ /K) and excellent thermomechanical properties in the red and near-infrared band of 700–800 nm [5–7].

The fluorescence spectrum of an alexandrite crystal with a Cr³⁺-doped concentration of 0.22 is measured by a fluorescence spectrometer (Edinburgh Instruments, Livingston, UK, FLS980), as shown in Figure 1. The strongest peak at 680 nm corresponds to the radiative transition of ²E(R_{1/2}) → ⁴A₂, which belongs to the three-level system. The line at 680 nm has a high pump threshold and low conversion efficiency, so it is difficult to oscillate at 680 nm at room temperature. The radiative transition at 700–820 nm belongs to the four-level system with a lower pump threshold and higher conversion efficiency [8,9]. Up to now, the four level system at 700–820 nm is the research focus in the laser field [5]. In 2019, Tawy G. reported a tunable and dual wavelength alexandrite laser [10]. The dual-wavelength is operated at 750.1 nm and 762.1 nm with wavelength separation of 12 nm. In 2020, Guan C. demonstrated dual-wavelength operation at 755.2 nm and 764.2 nm based on a 6 mm BRF [11]. Dual-wavelength lasers have been applied extensively in many fields, such as lidar, nonlinear frequency conversion and precision laser spectroscopy. It can also generate THz-wave light by using the differential frequency technique, which has been a research topic of laser technology in recent years.



Citation: Lin, H.; Bao, S.; Liu, X.; Song, S.; Wen, Z.; Sun, D. Dual-Wavelength Continuous-Wave and Passively Q-Switched Alexandrite Laser at 736.7 nm and 752.8 nm. *Photonics* **2022**, *9*, 769. <https://doi.org/10.3390/photonics9100769>

Received: 20 September 2022

Accepted: 12 October 2022

Published: 14 October 2022

Publisher's Note: MDPI stays neutral with regard to jurisdictional claims in published maps and institutional affiliations.



Copyright: © 2022 by the authors. Licensee MDPI, Basel, Switzerland. This article is an open access article distributed under the terms and conditions of the Creative Commons Attribution (CC BY) license (<https://creativecommons.org/licenses/by/4.0/>).

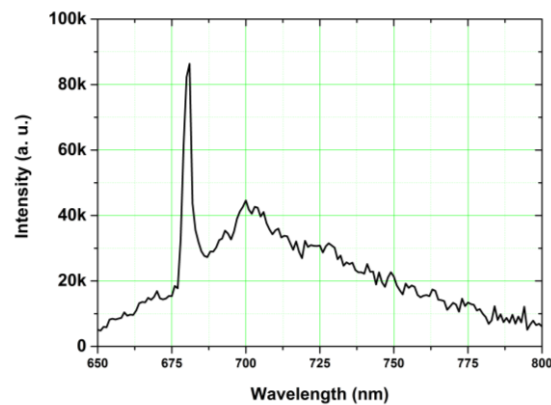


Figure 1. Fluorescence spectrum of an alexandrite crystal (c axis (001), 0.22% Cr³⁺-doped concentration and 15 °C).

The passively Q-switched technology is an important way to achieve a compact-ns laser pulse, and the SA plays the most critical role in this pulsed operation mode. The SA has typical nonlinear absorption characteristics. In the passively Q-switched laser system, the SA modulates the Q parameter of the laser cavity. When the SA absorption is unsaturated, the Q parameter is relatively low, and the energy is accumulated in the gain medium. With the increase in cavity energy, the SA absorption becomes saturated, and the Q parameter rapidly increases. At the same time, the energy accumulated in the gain medium is effectively extracted to form a strong pulse. In recent years, some novel SA nanomaterials with nonlinear absorption have been greatly developed, such as graphene; transition metal dichalcogenides/selenides (MoS₂, WS₂, WSe₂, MoSe₂, etc.); topological insulators and carbon nanotubes [12]. The SA characteristics of graphene have accelerated the fast development of 2D SA materials. However, there are some limits in the graphene SA due to its zero bandgap feature, such as weak linear absorption and small modulation depth. Fortunately, these limits are made up by the novel transition metal dichalcogenides (TMDs) due to their adjustable energy band gap, high carrier mobility and high nonlinear sensitivity [13].

With the development of the 2D material, TMDs, especially MoS₂, have gained great performances and widespread applications in the aspects of light sources, detectors, modulators and other optoelectronic devices [14]. However, there are still many novel areas that required further exploration for 2D TMDCs based on their nonlinear optical properties, particularly about their nonlinear optoelectronic characteristics in the visible, near-infrared, mid-infrared and other long-wavelength regions [15]. The studies in these areas will not only help to figure out the new electronic and optoelectronic effects of 2D TMDCs but also expand the research scope of 2D materials.

In this paper, by inserting a MoS₂ SA into the short resonator of the alexandrite laser, stable passively Q-switched operations at 736.7 nm and 752.8 nm can be generated. The narrowest pulse width is 154 ns with a repetition rate of 249 kHz.

2. Experimental Set-Up

The experimental setup is shown in Figure 2. A simple and compact plano–plano resonator with a short length of 18 mm is consisted of an input mirror (Mi) and an output coupler (Oc). A fiber-coupled red laser diode (LD) with multiple longitudinal modes and the central emission wavelength of 634.4 nm is used as a pump source. The fiber core diameter is 200 μm, and the numerical aperture is 0.22. The linear-polarized pump light passes through a focusing lens system and focuses to the left end face of an alexandrite crystal. The spot diameter is about 100 μm. The polarization extinction ratio (PER) of the CW linear-polarized pump light is about 20.5 dB. The alexandrite crystal has the dimensions of 4 × 4 × 4 mm³ and the Cr³⁺-doped concentration of 0.22. The crystal is wrapped in indium foil and cooled by water. The crystal temperature can be changed from 10 °C to

75 °C. Both sides of the alexandrite crystal are coated with antireflective (AR) coating at 634–800 nm ($T_{634-800} > 97\%$). Mi is coated with high transmittance (HT) coating at 634.4 nm ($T_{634.4} > 98\%$) and high reflectivity (HR) coating at 730–755 nm ($R_{730-755} > 99.8\%$). Oc has low transmittance at 730–755 nm ($T_{730-755} = 2\%$). M is a beam splitter, and the output light is divided into two channels.

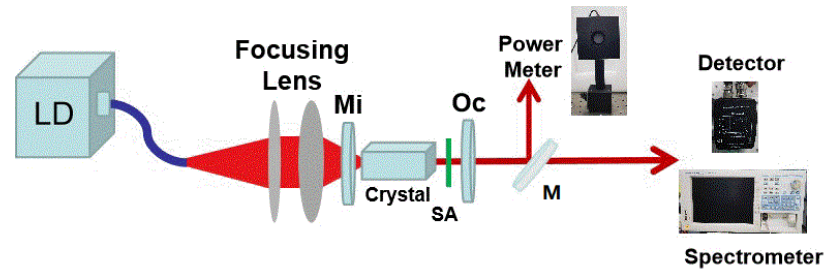


Figure 2. Dual-wavelength alexandrite laser at 736.7 nm and 752.8 nm.

The few-layer MoS₂ used in this experiment is prepared by chemical vapor deposition (CVD). When the pressure is about 1 atm pressure, the mass of S is more than 1 g, the gas flow is 30 sccm, the growth temperature is more than 700 °C and the growth time is 20 min, a MoS₂ thin film with an area of 10 × 10 mm² is grown on sapphire substrate. This MoS₂ film is a polycrystalline 2D material with about five layers. Then, this film is transferred to a fused quartz sheet as a transmissive SA. The fused quartz with a geometric thickness of 0.3 mm is also used as a FP etalon. It is widely known that the smaller thickness of the etalon thickness, the better effect of the frequency selection.

The transmitted spectrum of the MoS₂ SA is measured by a multifunctional spectrometer (Hong-Ming, New Taipei City, China, MFS-630) in Figure 3. The transmittance of the MoS₂ SA at 736.7 and 752.8 nm are 89.6% and 90.4%, respectively. Therefore, the line absorption of the MoS₂ SA at 736.7 and 752.8 nm are about 10.4% and 9.6%, respectively.

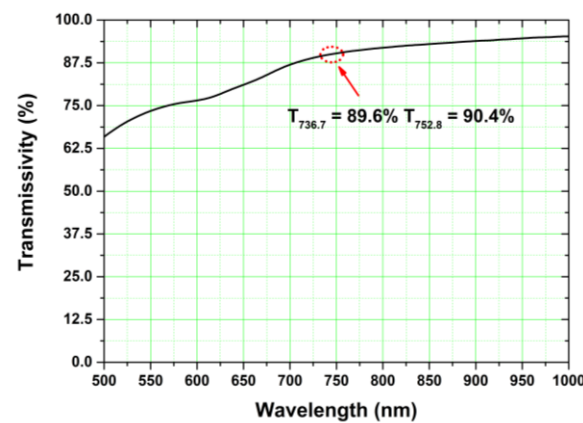


Figure 3. The transmitted spectrum of the MoS₂ SA.

Pulse profile and pulse train are measured by a high-speed detector (Thorlabs, Newton, NJ, USA, PDA10A2) and an oscilloscope (Tektronix, Beaverton, OR, USA, MDO4054-3). The bandwidth of the oscilloscope is 3 GHz. The output power, the light polarization and the output spectrum are detected by a polarimeter (Thorlabs PAX1000IR1), a thermal power meter (Thorlabs S314C) and a spectrometer (Yokogawa, Musashino, Tokyo, Japan, AQ6370), respectively.

3. Results and Discussion

3.1. CW Dual-Wavelength Laser at 736.7 nm and 752.8 nm

Since the temperature of the alexandrite crystal can affect the fluorescence lifetime of the upper energy level ⁴T₂ and the effective emission cross-section, we can obtain effective

laser output by controlling the temperature [5]. When the crystal temperature is controlled to 15 °C, the dual-wavelength output is observed in Figure 4. The pump threshold at 634.4 nm is about 1.94 W. Increasing the linear-polarized pump power at 634.4 nm, the output power accordingly increases, with the slope efficiency of 28.7%. At the maximal linear-polarized pump power of 5.44 W, the maximal output power reaches 1014 mW with the optical-to-optical conversion efficiency of 18.6%.

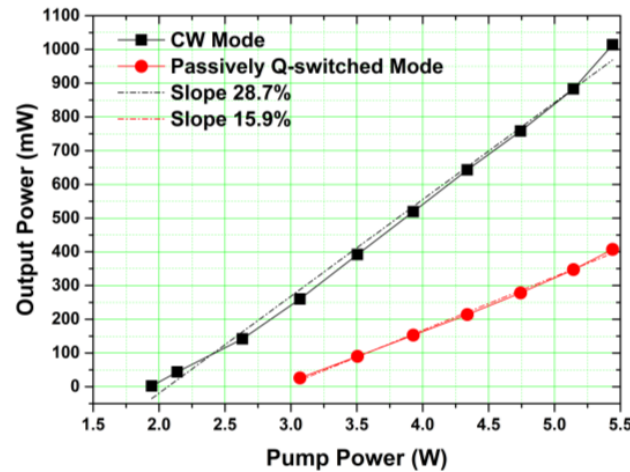


Figure 4. The output power of the dual-wavelength alexandrite laser at 736.7 nm and 752.8 nm.

Figures 5 and 6 display the detected and fine spectrum of the CW dual-wavelength alexandrite laser at the linear-polarized pump power of 5.44 W and the temperature of 15 °C. Two wavelength lines are simultaneously detected at 736.7 nm and 752.8 nm, which are approximately consistent with the alexandrite crystal’s fluorescence spectrum. During all the dual-wavelength CW mode, the separation difference between the two wavelengths is quite stable at about 16.1 nm. The relative intensities between the two lines are nearly equal, and the relative powers do not stay constant with a slight jitter due to the mode competition. The output laser is linearly polarized, which is the same as that of the linear-polarized pump source.

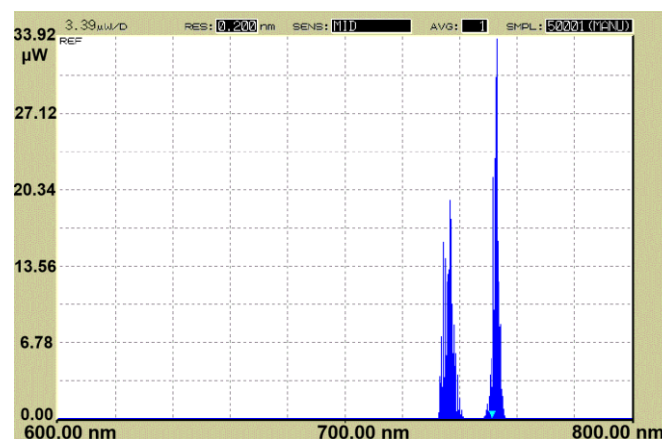


Figure 5. The detected spectrum of the CW dual-wavelength alexandrite laser at 736.7 nm and 752.8 nm.

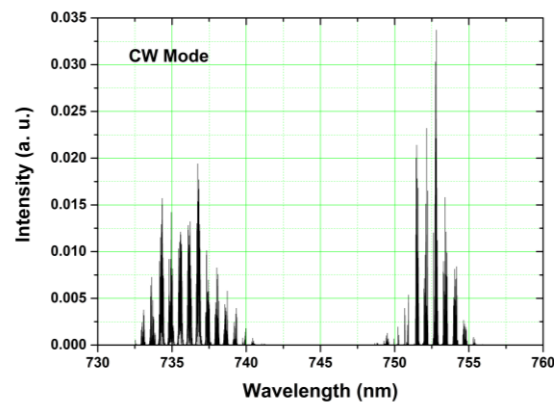


Figure 6. The fine spectrum of the CW dual-wavelength alexandrite laser at 736.7 nm and 752.8 nm.

The first line has the central wavelength of 736.7 nm with a wide line width of 3.9 nm. The first line with more than 12 longitudinal modes spans ~ 7.89 nm, from 732.58 to 740.47 nm. The average frequency difference between the two adjacent longitudinal modes is 3.40×10^{11} Hz, which matches the theoretical value of 3.43×10^{11} Hz of the SA FP etalon. The second line has the central wavelength of 752.8 nm with a wide line width of 3.3 nm. The second line with more than 10 longitudinal modes spans ~ 6.60 nm, from 748.78 to 755.38 nm. The average frequency difference is 3.46×10^{11} Hz. This dual-wavelength laser can be used to generate a 8.71-THz wave source based on a suitable nonlinear optical crystal.

3.2. Pulsed Dual-Wavelength Laser at 736.7 nm and 752.8 nm

Then, the pulsed dual-wavelength alexandrite laser is further studied by the MoS₂ SA. The output power is also shown in Figure 4. The linear-polarized pump threshold at 634.4 nm reaches 3.05 W due to the inserted loss of the MoS₂ SA. The largest output power is 407 mW, with a slope efficiency of 15.9%. The optical-to-optical conversion efficiency falls to 7.5%. The PER of the CW and pulsed dual-wavelength alexandrite laser is more than 26.9 dB.

Figure 7 displays the fine spectrum of the pulsed dual-wavelength alexandrite laser at the linear-polarized pump power of 5.44 W and a temperature of 13 °C. As mentioned above, the dual-wavelength operating at 736.7 nm and 752.8 nm is also simultaneously generated. However, the relative strength of these two lines changes, the first line at 736.7 nm is weakened, and the second line at 752.8 nm is strengthened. The first line at 736.7 nm with more than six longitudinal modes spans ~ 3.36 nm, from 735.00 to 738.36 nm. The line width of the first line is about 1.7 nm. Compared with that of the CW mode, the line width gets narrower. The second line at 752.8 nm with more than 13 longitudinal modes spans ~ 7.95 nm, from 749.49 to 757.44 nm. The line width of the second line is about 4.0 nm. Compared with that of the CW mode, the line width becomes wider. In the passively Q-switched mode, within the adequate storage energy time (~ 262 μ s) of the alexandrite crystal, the pump source can excite Cr³⁺ ions more sufficiently to the high energy level (⁴T₂), so that the stimulated emission at 752.8 nm is easier to stimulate [16].

Obviously, the intensity ratio between 736.7 nm and 752.8 nm in the CW and Q-switched mode are different. The cause of this phenomenon is the different insertion loss of the MoS₂ SA at 736.7 and 752.8 nm. Compared with the line at 736.7 nm, the line at 752.8 nm has a lower insertion loss of 9.6%, so the light intensity at 752.8 nm is higher.

A typical pulse diagram at the linear-polarized pump power of 5.44 W is shown in Figure 8, and the pulse width, i.e., the full width at half-maximum (FWHM), is 154 ns. The intensity stability of the pulse diagram is excellent due to the good saturation absorption characteristics of the MoS₂ SA.

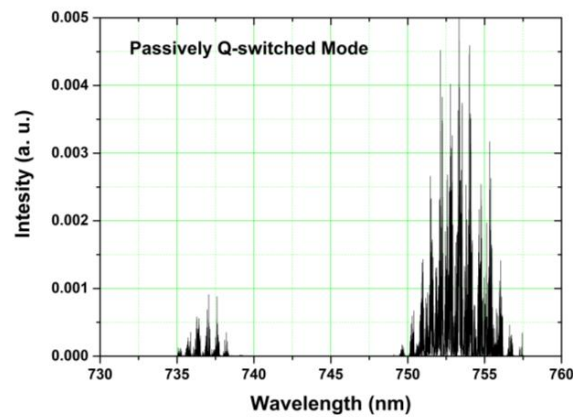


Figure 7. The fine spectrum of the dual-wavelength passively Q-switched alexandrite laser at 736.7 nm and 752.8 nm.

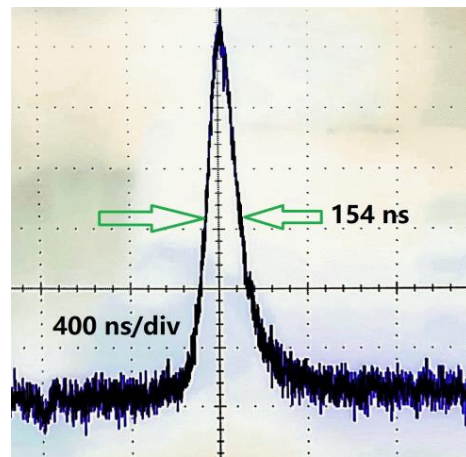


Figure 8. The pulse diagram of the alexandrite laser at 736.7 nm and 752.8 nm (154 ns).

Figure 9 represents the variations of the repetition rate and the pulse width with the linear-polarized pump power of the pulsed dual-wavelength laser at 736.7 nm and 752.8 nm. The repetition rate is increased from 79 kHz to 249 kHz, while the pulse width is reduced from 270 ns to 154 ns, as the linear-polarized pump power varies from 3.07 W to 5.44 W. The narrowest pulse width is only 154 ns, which is much lower than that reported in the references [10,17–19]. The calculated pulse energy varies from 0.33 μ J to 1.63 μ J, and the calculated peak power changes from 1.22 W to 10.6 W, as shown in Figure 10. The largest pulse energy and the maximal peak power are 1.63 μ J and 10.6 W, respectively.

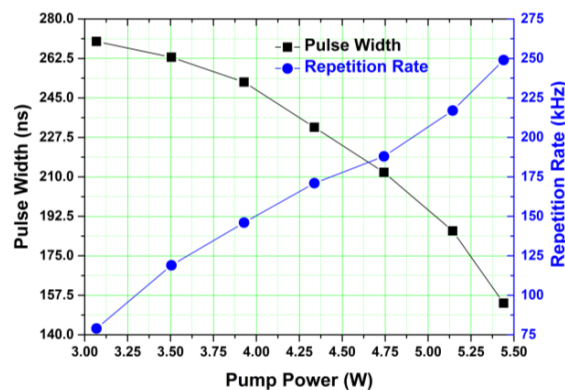


Figure 9. The repetition rate and pulse width of the alexandrite laser at 736.7 nm and 752.8 nm as a function of the pump power.

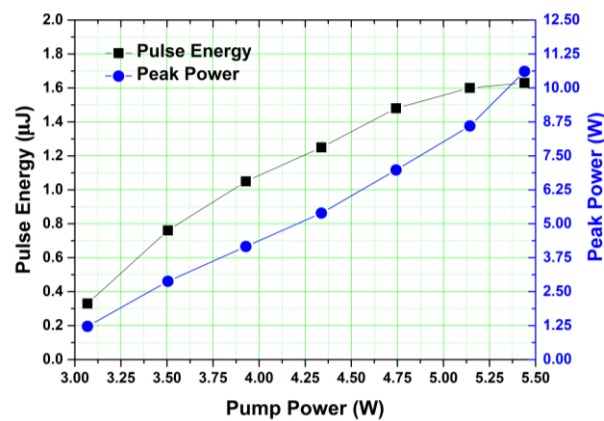


Figure 10. The pulse energy and peak power of the alexandrite laser at 736.7 nm and 752.8 nm as a function of the pump power.

Table 1 lists the performances of several lasers passively Q-switched by the MoS₂ SA [12,20–25]. We can see that, in contrast to other lasers at 946–2275 nm, the output performance of this dual-wavelength alexandrite laser at 736.7 nm and 752.8 nm is admirable and efficient. The MoS₂ SA demonstrate an ultra-broad saturable absorption range that covers the visible, near-infrared and mid-infrared spectral regions.

Table 1. The performances of several lasers passively Q-switched by the MoS₂ SA.

Gain Medium	Wavelength (nm)	Pulse Width	Repetition Rate (KHz)	Peak Power (W)	Reference
alexandrite	736.7, 752.8	154 ns	249	10.6	Here
Nd:YAG	946	208 ns	609	1.23	[20]
Yb:LuPO ₄	1010.5	61 ns	870	28.8	[21]
	1020.8	83 ns	429	57.8	
Yb:YAB	1039.6	99 ns	858	26.3	[22]
Er-fiber	1559.42	1.93 µs	73.96	1.55	[23]
Tm:YLF	1905.9	3.1 µs	76	27.5	[24]
Tm,Ho:YAP	2129	435 ns	55	11.3	[25]
Tm:YAP	2275	316 ns	228	5.53	[12]

4. Conclusions

In this paper, a good performance of dual-wavelength continuous-wave and passively Q-switched alexandrite laser operating at 736.7 nm and 752.8 nm is investigated. A simple and compact plano–plano resonator is chosen and a MoS₂ SA is applied to achieve the passively Q-switched operation. In the CW mode, the maximum output power is 1014 mW at the linear-polarized pump power of 5.44 W. The wide line width of the first line at 736.7 nm is 3.9 nm, while the wide line width of the second line at 752.8 nm is 3.3 nm. In the pulsed operation mode, the relative strength of these two lines changes; the first line at 736.7 nm is weakened, and the second line at 752.8 nm is strengthened. The line widths of the two lines at 736.7 nm and 752.8 nm are 1.7 nm and 4.0 nm, respectively. The narrowest pulse width and the maximal peak power of the dual-wavelength alexandrite laser are 154 ns and 10.6 W, respectively.

The output dual-wavelength spectrum peaked at 736.7 nm and 752.8 nm with the spectral spacing of 16.1 nm is obtained, which can be used to generate 8.71 THz-wave light based on a suitable nonlinear optical crystal.

Author Contributions: Conceptualization, H.L., S.B., X.L. and D.S.; methodology, H.L., S.B., S.S. and Z.W.; software, H.L.; validation, H.L. and S.B.; formal analysis, S.B., S.S. and Z.W.; investigation, X.L. and H.L.; resources, H.L. and D.S.; data curation, S.S. and Z.W.; writing—original draft preparation, H.L. and X.L.; writing—review and editing, H.L. and X.L.; visualization, S.S. and Z.W.; supervision, H.L. and X.L.; project administration, H.L.; funding acquisition, H.L. and D.S. All authors have read and agreed to the published version of the manuscript.

Funding: This paper was sponsored by the Natural Science Foundation of Fujian Province (Grants No. 2021J011217 and No. 2021I0025) and Science Technology Innovation of Xiamen (Grant No. 2022CXY04012).

Institutional Review Board Statement: Not applicable.

Informed Consent Statement: Not applicable.

Data Availability Statement: The data used to support the findings of this study are available from the corresponding author upon request.

Conflicts of Interest: The authors declare no conflict of interest.

References

1. Liu, X.; Zeng, X.-T.; Shi, W.-J.; Bao, S.-F.; Yu, T.; Lin, H.-Y. Application of a novel Nd: YAG/PPMgLN laser module speckle-suppressed by multi-mode fibers in an exhibition environment. *Photonics* **2022**, *9*, 46. [\[CrossRef\]](#)
2. Demirbas, U. Cr: Colquiriite lasers: Current status and challenges for further progress. *Prog. Quantum Electron.* **2019**, *68*, 100227. [\[CrossRef\]](#)
3. Munk, A.; Strotkamp, M.; Jungbluth, B.; Froh, J.; Mense, T.; Mauer, A.; Höffner, J. Rugged diode-pumped Alexandrite laser as an emitter in a compact mobile lidar system for atmospheric measurements. *Appl. Opt.* **2021**, *60*, 4668–4679. [\[CrossRef\]](#) [\[PubMed\]](#)
4. Ayatollahi, A.; Samadi, A.; Rajabi-Estarabadi, A.; Yadangi, S.; Nouri, K.; Firooz, A. Comparison of efficacy and safety of a novel 755-nm diode laser with conventional 755-nm alexandrite laser in reduction of axillary hairs. *Lasers Med. Sci.* **2020**, *35*, 373–378. [\[CrossRef\]](#) [\[PubMed\]](#)
5. Demirbas, U.; Kärtner, F.X. Alexandrite: An attractive thin-disk laser material alternative to Yb:YAG? *J. Opt. Soc. Am. B* **2020**, *37*, 459–472. [\[CrossRef\]](#)
6. Song, Y.; Wang, Z.-M.; Bo, Y.; Zhang, F.-F.; Zhang, Y.-X.; Zong, N.; Peng, Q.-J. 2.55 W continuous-wave 378 nm laser by intracavity frequency doubling of a diode-pumped Alexandrite laser. *Appl. Opt.* **2021**, *60*, 5900–5905. [\[CrossRef\]](#) [\[PubMed\]](#)
7. Walochnik, M.; Jungbluth, B.; Huber, H.; Ammersbach, J.; Munk, A.; Strotkamp, M.; Traub, M.; Hoffmann, D.; Poprawe, R. Diode-pumped cw Alexandrite laser with temporally stable 6.5 W in TEM₀₀ operation with prospect of power scaling. *Opt. Express* **2020**, *28*, 15761–15769. [\[CrossRef\]](#) [\[PubMed\]](#)
8. Coney, A.T.; Damzen, M.J. High-energy diode-pumped alexandrite amplifier development with applications in satellite-based lidar. *J. Opt. Soc. Am. B* **2021**, *38*, 209–219. [\[CrossRef\]](#)
9. Moon, B.; An, Y.J.; Kim, Y.S.; Lee, J.H.; Ju, B.-K.; Jhon, Y.M. Cavity-dumped mode-locked Alexandrite laser oscillator with 100 mJ pulses stabilized by using a double trigger system. *Opt. Express* **2022**, *30*, 3516–3523. [\[CrossRef\]](#) [\[PubMed\]](#)
10. Tawy, G.; Damzen, M.J. Tunable, dual wavelength and self-Q-switched Alexandrite laser using crystal birefringence control. *Opt. Express* **2019**, *27*, 17507–17520. [\[CrossRef\]](#) [\[PubMed\]](#)
11. Guan, C.; Liu, Z.; Cong, Z.; Wang, S.; Nie, Y.; Zhang, L.; Zhu, Z.; Qi, Y.; Zhang, X.; Zhao, Z. Alexandrite laser on-peak pumped by a frequency doubled Raman Yb-fiber laser at 589 nm. *OSA Contin.* **2020**, *3*, 1204–1210. [\[CrossRef\]](#)
12. Zha, F.; Chu, H.; Pan, Z.; Pan, H.; Zhao, S.; Yang, M.; Li, D. Large-scale few-layered MoS₂ as a saturable absorber for Q-switching operation at 2.3 μm. *Opt. Lett.* **2022**, *47*, 3271–3274. [\[CrossRef\]](#) [\[PubMed\]](#)
13. Ahmed, M.H.M.; Latiff, A.A.; Arof, H.; Ahmad, H.; Harun, S.W. Femtosecond mode-locked erbium-doped fiber laser based on MoS₂-PVA saturable absorber. *Opt. Laser Technol.* **2016**, *82*, 145–149. [\[CrossRef\]](#)
14. Cong, W.; Jie, L.; Han, Z. Ultrafast pulse lasers based on two-dimensional nanomaterials. *Acta Phys. Sin.* **2019**, *68*, 188101.
15. Debnath, P.C.; Yeom, D.-I. Ultrafast fiber lasers with low-dimensional saturable absorbers: Status and prospects. *Sensors* **2021**, *21*, 3676. [\[CrossRef\]](#)
16. Lin, H.-Y.; Guo, J.; Ning, D.-Y.; Wang, S.-W.; Tan, H.-M. LD end-pumped intracavity frequency doubled Yb:YAG laser. *Opt. Commun.* **2008**, *281*, 6065–6067. [\[CrossRef\]](#)
17. Parali, U.; Sheng, X.; Minassian, A.; Tawy, G.; Sathian, J.; Thomas, G.M.; Damzen, M.J. Diode-pumped Alexandrite laser with passive SESAM Q-switching and wavelength tunability. *Opt. Commun.* **2018**, *410*, 970–976. [\[CrossRef\]](#)
18. Munk, A.; Jungbluth, B.; Strotkamp, M.; Hoffmann, H.-D.; Poprawe, R.; Höffner, J.; Lübken, F.-J. Diode-pumped alexandrite ring laser in single-longitudinal mode operation for atmospheric lidar measurements. *Opt. Express* **2018**, *26*, 14928–14935. [\[CrossRef\]](#)
19. Munk, A.; Strotkamp, M.; Walochnik, M.; Jungbluth, B.; Traub, M.; Hoffmann, H.-D.; Poprawe, R.; Höffner, J.; Lübken, F.-J. Diode-pumped Q-switched Alexandrite laser in single longitudinal mode operation with Watt-level output power. *Opt. Lett.* **2018**, *43*, 5492–5495. [\[CrossRef\]](#)

20. Lin, H.; Zhu, W.; Xiong, F.; Cai, L. MoS₂-based passively Q-switched diode-pumped Nd:YAG laser at 946 nm. *Opt. Laser Technol.* **2017**, *91*, 36–39. [[CrossRef](#)]
21. Dou, X.; Yang, J.; Zhu, M.; Xu, H.; Han, W.; Zhong, D.; Teng, B.; Liu, J. Watt-level passively Q-switched Yb:LuPO₄ miniature crystal laser with few-layer MoS₂ saturable absorber. *Opt. Express* **2018**, *26*, 14232–14240. [[CrossRef](#)] [[PubMed](#)]
22. Cao, S.; Wang, L.; Dong, L.; Han, W.; Liu, J. Efficient operation of an Yb:YAl₃(BO₃)₄ laser passively Q-switched with 2D MoS₂ saturable absorber. *J. Russ. Laser Res.* **2021**, *42*, 87–94. [[CrossRef](#)]
23. Ahmad, H.; Soltani, S.; Thambiratnam, K. Q-switched erbium-doped fiber laser with molybdenum disulfide (MoS₂) nanoparticles on D-shaped fiber as saturable absorber. *J. Nonlinear Opt. Phys.* **2019**, *28*, 1950026. [[CrossRef](#)]
24. Li, L.; Yang, X.; Zhou, L.; Xie, W.; Xu, C.; Wang, Y.; Shen, Y.; Lv, Z.; Duan, X.; Lu, Y. High beam quality passively Q-switched operation of a slab Tm:YLF laser with a MoS₂ saturable absorber mirror. *Opt. Laser Technol.* **2019**, *112*, 39–42. [[CrossRef](#)]
25. Luan, C.; Zhang, X.; Yang, K.; Zhao, J.; Zhao, S.; Li, T.; Qiao, W.; Chu, H.; Qiao, J.; Wang, J.; et al. High peak power passively Q-switched 2 μm laser with MoS₂ saturable absorber. *IEEE J. Sel. Top. Quantum Electron.* **2017**, *23*, 66–70. [[CrossRef](#)]